Int J Appl Earth Obs Geoinformation 84 (2020) 101959

Contents lists available at ScienceDirect

Int J Appl Earth Obs Geoinformation

journal homepage: www.elsevier.com/locate/jag

Wall-to-wall spatial prediction of growing stock volume based on Italian National Forest Inventory plots and remotely sensed data

Gherardo Chirici[a], Francesca Giannetti[a], Ronald E. McRoberts[b,c], Davide Travaglini[a], Matteo Pecchi[a], Fabio Maselli[d], Marta Chiesi[d], Piermaria Corona[e]

[a] Dipartimento di Scienze e Tecnologie Agrarie, Alimentari, Ambientali e Forestali, Università degli Studi di Firenze, 50145, Firenze, Italy
[b] Department of Forest Resources, University of Minnesota, Saint Paul, MN, 55108, USA
[c] Northern Research Station, U.S. Forest Service, Saint Paul, MN, 55108, USA
[d] CNR-IBE, Via Madonna del Piano, 10, 50019, Sesto Fiorentino, FI, Italy
[e] CREA, Research Centre for Forestry and Wood, viale Santa Margherita 80, 52100, Arezzo, Italy

ARTICLE INFO

Keywords:
National Forest Inventory
Spatial estimation
Growing stock
Landsat
Italy
Growing stock volume

ABSTRACT

Spatial predictions of forest variables are required for supporting modern national and sub-national forest planning strategies, especially in the framework of a climate change scenario. Nowadays methods for constructing wall-to-wall maps and calculating small-area estimates of forest parameters are becoming essential components of most advanced National Forest Inventory (NFI) programs. Such methods are based on the assumption of a relationship between the forest variables and predictor variables that are available for the entire forest area. Many commonly used predictors are based on data obtained from active or passive remote sensing technologies. Italy has almost 40% of its land area covered by forests. Because of the great diversity of Italian forests with respect to composition, structure and management and underlying climatic, morphological and soil conditions, a relevant question is whether methods successfully used in less complex temperate and boreal forests may be applied successfully at country level in Italy.

For a study area of more than 48,657 km^2 in central Italy of which 43% is covered by forest, the study presents the results of a test regarding wall-to-wall, spatially explicit estimation of forest growing stock volume (GSV) based on field measurement of 1350 plots during the last Italian NFI. For the same area, we used potential predictor variables that are available across the whole of Italy: cloud-free mosaics of multispectral optical satellite imagery (Landsat 5 TM), microwave sensor data (JAXA PALSAR), a canopy height model (CHM) from satellite LiDAR, and auxiliary variables from climate, temperature and precipitation maps, soil maps, and a digital terrain model.

Two non-parametric (random forests and k-NN) and two parametric (multiple linear regression and geographically weighted regression) prediction methods were tested to produce wall-to-wall map of growing stock volume at 23-m resolution. Pixel level predictions were used to produce small-area, province-level model-assisted estimates. The performances of all the methods were compared in terms of percent root mean-square error using a leave-one-out procedure and an independent dataset was used for validation. Results were comparable to those available for other ecological regions using similar predictors, but random forests produced the most accurate results with a pixel level $R^2 = 0.69$ and $RMSE_{\%} = 37.2\%$ against the independent validation dataset. Model-assisted estimates were more precise than the original design-based estimates provided by the NFI.

1. Introduction

Forest data are essential for multiple purposes including international and national forest monitoring programs, reporting and assessing forest resource distribution (e.g. Kyoto protocol) (Corona et al., 2011; FAO, 2010), monitoring biodiversity (Chirici et al., 2012; FOREST EUROPE, 2015), improving restoration programs (FAO and UNCCD, 2015; Smith et al., 2016) and managing at local scales to improve decision-making processes, silvicultural measures, harvesting and conservation activities.

Usually, in the context of international and national programs, this type of data is collected using sample-based National Forest Inventories (NFIs) that are designed to provide aggregated estimates of forest parameters such as forest area, growing stock volume, biomass, increments at national and regional levels (Brosofske et al., 2014; Kangas et al., 2018). These aggregated statistics are essential to support decision-making processes and to develop strategies over large areas only, because they just provide limited explicit geographic spatial detail, such as large sub-national regions. In these traditional NFIs, remote sensing is used for purposes such as initial stratification of sampling units

https://doi.org/10.1016/j.jag.2019.101959
Received 17 May 2019; Received in revised form 8 August 2019; Accepted 2 September 2019
Available online 03 October 2019

according to their main land uses, most commonly through the use of fine resolution remotely sensed imagery (McRoberts et al., 2009, McRoberts et al., 2010a,b; Corona, 2010).

In countries characterized by longer NFI traditions and/or stronger interests in the operational implementation of sustainable forest management practices such as in Sweden, Finland, Denmark (Næsset et al., 2004; Nord-Larsen and Schumacher, 2012; Tomppo et al., 2008), Canada (Boudreau et al., 2008; Matasci et al., 2018), Austria (Hollaus et al., 2009) and Switzerland (Waser et al., 2017, 2015), traditional inventories are now integrated with a more advanced use of remote sensing technology for mapping forest variables (McRoberts and Tomppo, 2007).

Most frequently these methods are applied to construct wall-to-wall spatial estimates of forest variables such as growing stock volume (Nilsson et al., 2017; Nord-Larsen and Schumacher, 2012), biomass (Nord-Larsen and Schumacher, 2012), forest cover (Waser et al., 2015), or forest changes (Næsset et al., 2013).

Wall-to-wall forest mapping in these modern forest inventories, sometimes characterized as Enhanced Forest Inventories (EFI) (Stinson and White, 2018), is considered an essential component of the forest inventory project aimed at producing forest parameter estimates at multiple spatial scales: traditional aggregated statistics useful for national planning, and at the same time, consistent small-area estimates for sub-national planning or even pixel-level raw data to support local forest management (Matasci et al., 2018; McRoberts et al., 2010a,b; Næsset et al., 2004; Nilsson et al., 2017; Tomppo et al., 2008; Waser et al., 2015).

The EFI approach produces a variety of benefits: it is able to provide detailed information to support decision-making and reduce the costs for numerous forest activities including silvicultural treatments (frequently in the framework of precision forestry), quantification of forest ecosystem services, wood harvesting, and conservation strategies (Kangas et al., 2018). The costs of the shift from a traditional NFI to an EFI are limited, because the major required investment, the field activity, remains the same or it may be even reduced if remote sensing is used for the optimization of the sampling strategy. Major costs may be related to the acquisition and elaboration of remotely sensed data.

Research activities carried out in the last 20 years demonstrated that 3D pulses from airborne laser scanning (ALS) are the most valuable data source for enhancing of growing stock volume and other forest structural variables estimates (Kangas et al., 2018; McRoberts et al., 2010a,b; Næsset, 2007; Nilsson et al., 2017; Montaghi et al., 2013; Nord-Larsen and Schumacher, 2012). The optimal option for the implementation of an EFI is thus the use of ALS data acquired in the same period as the field survey.

ALS acquisition is still expensive, but ALS data are useful for a vast array of applications in land planning, thus its cost can be shared among multiple stakeholders and agencies. However, wall-to-wall ALS data at country level are not yet available in several regions of Europe such as Italy (Giannetti et al., 2018b), Spain (Fernández-Landa et al., 2018), and most developing countries.

Together with ALS, or in case ALS is not available, satellite multispectral data can also be useful, with only small costs because they are nowadays available online for free. Barrett et al. (2016) reported in their review that when NFI data are linked with remotely sensed data, the most frequently used satellite systems are medium-resolution satellites with Landsat the most used. Medium-resolution satellite images (pixel size between 20 and 30 m) permit the prediction of forest variables with spatial detail relevant for forest inventories and sustainable forest management, and also as reported by Nilsson et al. (2017), for forest plans although forest agencies, forest companies, and forest owner associations would prefer as fine resolution as possible (in the range 10–30 m).

Several methods produce wall-to-wall maps of forest variables from field observations (Corona et al., 2014). Such methods are based on the assumption that a model of the relationship between the forest variables to be predicted and predictor variables that are available for the entire forest area can be constructed. These methods include both parametric (i.e. multiple linear regression, geographically weighted regression) and non-parametric (i.e. k-NN, random forests, Artificial Network Analysis) techniques (Barrett et al., 2016; Brosofske et al., 2014; Chirici et al., 2016; Moser et al., 2017) and have already been tested across different forest types and regions (Chirici et al., 2016).

All these methods have been widely applied with remote sensing-based predictors such as 3D data (from ALS data, microwave, or photogrammetry) (e.g. McRoberts et al., 2010a,b; Næsset, 2007; Nilsson et al., 2017; Nord-Larsen and Schumacher, 2012; Persson et al., 2017; Waser et al., 2017, 2015; Hobi and Ginzler, 2012; Ginzler and Hobi, 2015; Breidenbach and Astrup, 2012; Rahlf et al., 2014) or multispectral images from aerial, manned or unmanned, or satellite platforms, (e.g. Brosofske et al., 2014; Fernández-Landa et al., 2018; Matasci et al., 2018; Reese et al., 2002).

All these approaches have already become operational for boreal forests (Kangas et al., 2018), while in Mediterranean areas experiences are yet limited, most probably because wood production is economically less relevant and forest composition and structure is more complex, and thus more difficult to model.

Maselli et al. (2014) tested moderate resolution imagery from global 1 km resolution forest canopy height data from the Geoscience Laser Altimeter System (GLAS) onboard the ICES at satellite (Ice, Cloud, and land Elevation Satellite) for enhancing of growing stock volume estimates at country-level in Italy. Fernández-Landa et al. (2018) enhanced the estimates of the main forest inventory variables (i.e. stand density, basal area and growing stock volume) acquired in the Spanish NFI with Landsat images and ALS in a small study area in La Rioja (Spain). Condés and McRoberts (2017) developed an accurate method for updating NFI estimates of mean growing stock volume (m^3ha^{-1}) using models to predict annual plot-level volume change, and for estimating the associated uncertainties using four monospecific forest types and Landsat images for two study areas in Spain.

Mura et al. (2015) and Bottalico et al. (2017) used ALS for enhancing the estimates of structural diversity in different test areas in Italy (i.e. Molise, Tuscany and Sardinia) using remote sensing-base estimation, while Mura et al. (2018) used Sentinel-2 imagery to enhancing the estimates of growing stock volume for two test areas in Italy.

To our knowledge country-level experiences in Mediterranean areas have not yet been reported in the literature.

However, in Mediterranean areas there is an increasing need for wall-to-wall forest maps because these forests are considered more vulnerable to climate change scenarios and to natural and anthropogenic disturbances such as forest fires and urban sprawl (FAO, 2013; Scarascia-Mugnozza et al., 2000).

The current study aims at constructing wall-to-wall estimates of forest growing stock (GSV) for a large test area (i.e. 48,657 km^2) in central Italy by combining NFI plot data, remotely sensed and auxiliary variables. In particular, the research evaluated the most accurate imputation approach for mapping GSV at fine spatial resolution (23 × 23 m) and calculating small area estimates using a model-assisted approach. The results of this experimental test are aimed at identifying the optimal procedure for the operational GSV and biomass estimation at country-level in Italy.

2. Materials

2.1. Study area

To test possible wall-to-wall spatial estimation alternatives at country-level in Italy we selected a large region in central Italy including the whole of Tuscany and most of the Emilia-Romagna and part of the Liguria Regions for a total extent of 48,657 km^2 (Fig. 1). The area is characterized by large geographical and topographical variability from flat coastal areas, to gentle hills, to steep mountains with elevation

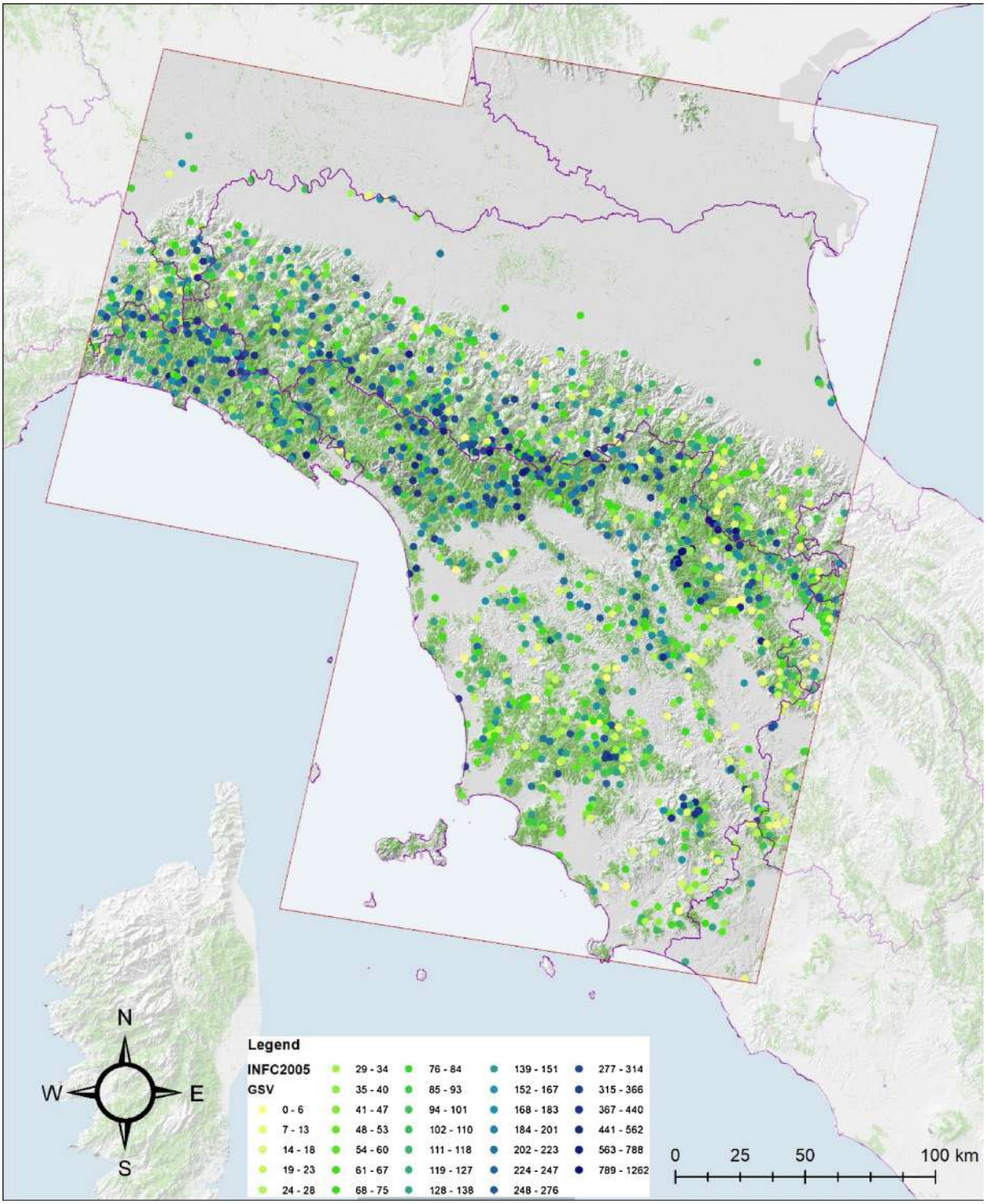

Fig. 1. Study area location (red boundary) and spatial distribution of NFI plots (INFC, 2004). Values of GSV in m^3 ha^{-1}. (For interpretation of the references to colour in this figure legend, the reader is referred to the web version of this article).

up to 2000 m a.s.l. Total precipitation per year ranges between 3000 mm in Alpi Apuane to 600 mm in the Maremma area (south of Tuscany), while mean temperature ranges from 6 °C in Abetone Mountain and Camaldoli to 17 °C along the coast.

Broadleaf species such as downy oak (*Quercus pubescens* Willd.), pedunculated oak (*Q. robur* L.), Turkey oak (*Q. cerris* L.) and sessile oak (*Q. petraea* Liebl.) (Pecchi et al., 2019) comprise 88% of the total forest area. The coppice management system is applied in 63% of the forests in the study area. Dominant coniferous species, mainly in artificial plantations, are maritime pine (*Pinus pinaster* Ait.) and black pine (*P. nigra* Arnold). Six out of the 14 European Forest Types (Barbati et al., 2014; Giannetti et al., 2018) are represented in the study area.

2.2. Italian national forest inventory data

The field reference data for the study area were acquired for 1350 plots measured in the framework of the 2nd Italian NFI (INFC, 2004) (Fig. 1) which is based on a three-phase, non-aligned, systematic

sampling design (Fattorini et al., 2006). Sampling units are located randomly within 1-km x 1-km grid cells, and in the first phase are classified on the basis of land use using aerial photos. For a subsample of the first-phase forest sampling units, qualitative information such as forest type, management, and property is collected during a terrestrial survey. For a subsample of the second-phase units, a quantitative survey is carried out in the field using circular 13 m radius plots (i.e., 530 m^2). The first two phases are aimed at estimating the forest area and classifying it into forest categories, while the third phase is aimed at collecting observations and measurements for biophysical variables. The plot data used for this study were acquired in the third phase (INFC, 2004). The plot geolocation available for this study has been the target coordinate of the sampling unit, i.e. the theoretical center of the plot that the field crew should reach. Several studies reported in the literature have evaluated the impact of inexact plot location for the estimation of forest growing stock volume or biomass. All of them relate to the use of Airborne Laser Scanning (ALS) pulses, which resulted to be very sensitive to plot location accuracy (McRoberts et al., 2018). On the other hand, in this study we predict the GSV for pixels of 23 m resolution and we expect that the error of Global Navigation Satellite System (GNSS) receivers should be much smaller than the pixel size and for this reason in this study we ignored potential positional inaccuracy of NFI plots.

For each field plot, the predicted GSV per hectare for all callipered trees is freely available online via a spatial database at https://www.inventarioforestale.org/ (Borghetti and Chirici, 2016; Pecchi et al., 2019). The GSV of each tree was predicted using species-specific allometric models developed in the framework of the NFI using tree DBH and tree height as independent variables (Tabacchi et al., 2011). The GSV per hectare of each plot was predicted as the aggregation of volume predictions for all the trees callipered in the plot. The uncertainty of allometric model predictions was considered negligible and ignored following previous results (McRoberts et al., 2016a,b). In Fig. 1 we report the spatial distribution of sample plots, while in Fig. 2 we report the GSV distribution for the 1350 field plots used in this study.

2.3. Validation data

To validate the results of our estimation we used independent field data from 332 circular plots for a different dataset, of which 297 plots of 1256.4 m^2 were measured between 2004 and 2009 to support forest management in forest areas in Tuscany and 35 are ICP level I circular plots measured in 2005 in the framework of the BioSoil Forest Biodiversity project (Galluzzi et al., 2019). The plots are representative of all forest types in the study area. The plots measured to support forest management activities are located in: Vallombrosa, Cerventosa, Lucignano, Chianti, Muraglione, Rincine and Cecina (Fig. 3).

The centers of these plots were georeferenced using a Trimble Juno 3B GNSS system and post-processed with sub-meter accuracy with the closest GNSS national base station and for each plot we applied the same field protocol developed for the Italian INFC. The GSV of each tree and the GSV per hectare of the validation plots were predicted using the same approach described in the previous paragraph for INFC plots. The GSVs of ICP BioSoil Forest Biodiversity plots were estimates using international allometric models as reported in Galluzzi et al. (2019).

The mean GSV in the validation dataset is 350.57 $m^3 ha^{-1}$, with a minimum of 6.8, a maximum of 1288.2 $m^3 ha^{-1}$ and a standard deviation of 254.79 $m^3 ha^{-1}$. The average GSV in the validation data is therefore consistently greater than the GSV registered in the INFC dataset. This was expected since the validation dataset is related to forests located in productive sites where the main forest management objective is nature and landscape conservation. This means that wood removals are generally less than the increments and the GSV tends to accumulate.

2.4. Predictor variables

The rationale for choosing the predictors is based on two elements: *i*) the availability for the whole Italy, since this test is aimed at evaluating different approaches for a country level wall-to-wall GSV spatial estimation, and *ii*) that the predictor can be at least potentially related to GSV from the results of previous investigations or from literature.

2.4.1. Remotely sensed variables

2.4.1.1. Landsat. After having evaluated other possible imagery (Chirici, 2019), to cover the study area we used imagery for three Landsat 5 Thematic Mapper (TM) scenes, 192,030 and 192,029 acquired the 23rd of June 2005, and an image for scene 193,029 acquired the 30th of June 2005. The three images are cloud-free for the forest part of the study area. Level-1 data products in Digital Numbers (DN) where transformed to top of atmosphere (TOA) radiance using

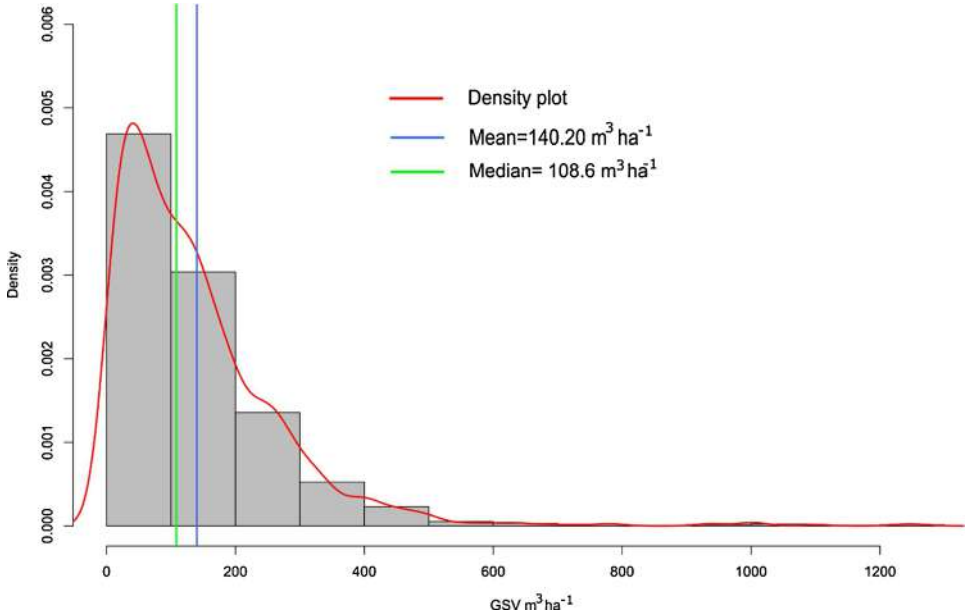

Fig. 2. GSV distribution measured in 1350 INFC plots. The red line is the density distribution, the green line is the median value and the blue line is the mean value. (For interpretation of the references to colour in this figure legend, the reader is referred to the web version of this article).

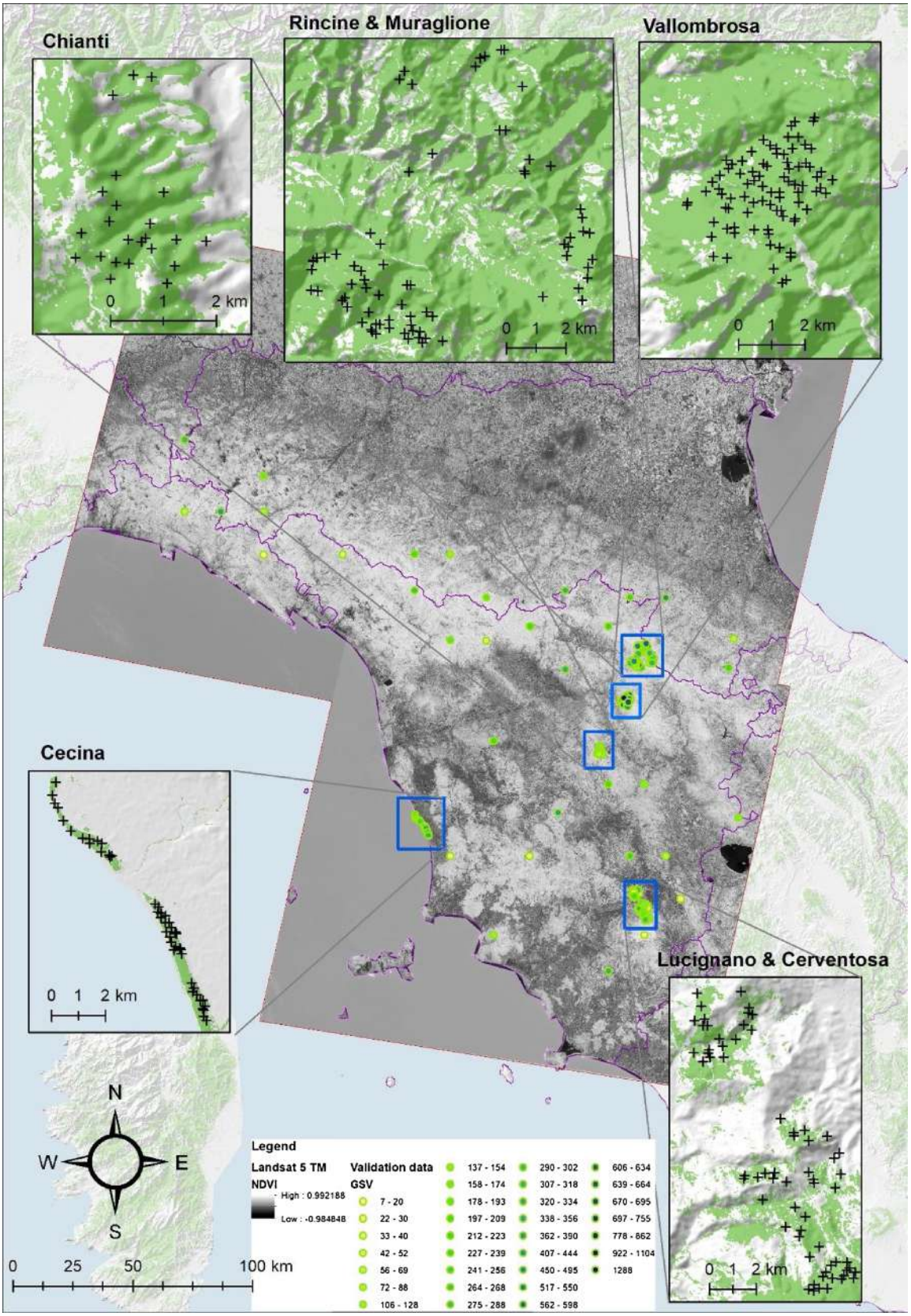

Fig. 3. Validation data used in the study on the basis of the Landsat 5 T M NDVI imagery.

Table 1
Predictors based on remotely sensing and auxiliary data used to predict GSV.

Spatial Database	Band/information	Name of predictors variables	Original spatial resolution
Landsat 5 T M	Band 1	Landsat_B1	30 m
Landsat 5 T M	Band 2	Landsat_B2	30 m
Landsat 5 T M	Band 3	Landsat_B3	30 m
Landsat 5 T M	Band 4	Landsat_B4	30 m
Landsat 5 T M	Band 5	Landsat_B5	30 m
Landsat 5 T M	Band 6	Landsat_B6	60 m
Landsat 5 T M	Band 7	Landsat_B7	30 m
Global PALSAR/PALSAR-2	HH polarization	SAR_HH	25 m
Global PALSAR/PALSAR-2	HV polarization	SAR_HV	25 m
TIN Italy	DTM	DTM	10 m
TIN Italy	SLOPE based on DTM	SLOPE	10 m
Regional land use/land cover map	Forest/non-Forest map	Forest mask	Vector 1:10.000
Climate data	Total annual precipitation	prec	1 km
Climate data	Mean annual temperature	temp_mean	1 km
Climate data	Maximum annual temperature	temp_max	1 km
Climate data	Minimum annual temperature	temp_min	1 km
European Soil Database v2.0	Subsoil available water capacity	AWC_SUB_P	1 km
European Soil Database v2.0	Topsoil available water capacity	AWC_TOP_P	1 km
European Soil Database v2.0	Volume of stones	VS_P	1 km
European Soil Database v2.0	Depth to rock	DR_P	1 km
European Soil Database v2.0	Subsoil cation exchange capacity	CEC_SUB_P	1 km
European Soil Database v2.0	Topsoil cation exchange capacity	CEC_TOP_P	1 km
European Soil Database v2.0	Soil exchange capacity	DIMP_P	1 km
Wall-to-wall Canopy Height Map	Mean Vegetation Height	CHM	1 km

radiometric rescaling coefficients provided with the Level-1 products (Fig. 3).

2.4.1.2. Global PALSAR/PALSAR-2. The SAR data used are the global 25 m resolution PALSAR-2/PALSAR mosaic available for the year 2007 as free open spatial dataset at Japanese Aerospace Exploration Agency (JAXA). Images are available as backscattering coefficient for each polarization HH and HV using the L-band Synthetic Aperture Radars (PALSAR and PALSAR-2) on Advanced Land Observing Satellite (ALOS) and Advanced Land Observing Satellite-2 (ALOS-2). The global 25 m resolution PALSAR/PALSAR-2 mosaic is processed for the geometric correction and radiometric correction to reduce topographic effects on image intensity (i.e. slope correction). The observation mode is FBD (HH, HV) and the off-nadir angle is 34.3 degrees.

2.4.2. Auxiliary variables

2.4.2.1. Digital elevation model. We used the 10 m resolution DEM TINITALY which is the finest and most accurate DEM currently available in Italy (Fornaciai et al., 2012; Tarquini et al., 2007; Tarquini and Nannipieri, 2017). TINITALY is available at http://tinitaly.pi.ingv.it/ in grid format.

2.4.2.2. Climate data. Climate data were derived from 1-km downscaled climatological surfaces released for Italy by Maselli et al. (2012). This dataset was obtained through application of geographically weighted regression to the Pan-European E-OBS database, which has a 0.25° spatial resolution (Haylock et al., 2008). The Italian dataset is representative for the period 1981–2010 and includes total annual rainfall and minimum and maximum temperatures, from which mean temperature was currently estimated. The downscaled E-OBS dataset over-estimates minimum temperature and under-estimates maximum temperature and, most importantly, rainfall (Maselli et al., 2012). For this reason we used a version of the rainfall dataset that was corrected as described in Fibbi et al. (2016).

2.4.2.3. Soil data. The soil data used were derived from the European Soil Database v2.0 (2004) (Panagos, 2006). This spatial dataset is the only geographically harmonized soil database available for Europe. It contains a soil geographic database (SGDBE) (i.e. polygons) to which a number of essential soil attributes are attached. From this database we used the quantitative information related to: (i) subsoil available water soil capacity; (ii) topsoil available water soil capacity; (iii) volume of stones; (iv) depth to rock; (v) subsoil cation exchange capacity; (vi) topsoil cation exchange capacity; (vii) soil exchange capacity.

2.4.2.4. World canopy height model. We used the vegetation height available in the wall-to-wall Canopy Height Map (Simard et al., 2011) estimated at 1-km spatial resolution from the ICESat GLAS.

2.4.3. Forest mask

A forest mask was needed to limit the spatial estimation to pixels with predicted forest land cover only. As far as possible the forest mask should mimic the same standard FAO definition used in the Italian NFI (INFC, 2004) and should be dated as close as possible to the reference year 2005 used for the acquisition of the inventory field plot data. After several tests we decided to use local fine resolution land use/land cover maps constructed at a 1:10,000 scale. We used maps from regional geoportals of Liguria, available for the year 2009 (https://geoportal.regione.liguria.it); Tuscany, available for the year 2007 (http://dati.toscana.it/dataset/ucs); and Emilia Romagna, available for the year 2008 (http://geoportale.regione.emilia-romagna.it). We rasterized the original fine resolution maps obtaining a 23 m resolution forest mask of approximately 21,327 km^2, 43% of the study area (Fig. 3).

3. Methods

Imputation methods facilitate prediction of a *response variable Y* measured for a sample of size *n* selected from a finite population of size N. X is used to denote a vector of auxiliary variables with observations for all population units.

The terminology developed for remote sensing applications in forest inventory may vary with respect to the estimation method. When regression models are used, the auxiliary variables are designated as *independent variables* and the response variable is the *dependent variable* (Mardia et al., 1979). For k-Nearest Neighbors (k-NN), the auxiliary variables are designated *feature variables* and the space defined by the feature variables is designated the *feature space;* the set of sample population units for which observations of both response and feature variables are available is designated the *reference set*; and the set of population units for which predictions of response variables are desired

is designated the *target set* (Chirici et al., 2016). For random forests, Breiman (2001) used the term *predictors* to denote the auxiliary variables.

The test area was tessellated into 23 × 23 m pixels whose size mimicked the area of the field plots measured in the field in the NFI program. All the predictors were resampled using a cubic convolution filter of 3 × 3 pixels to the final pixel of resolution of 23 m.

Thus, the population size of $N = 40{,}317{,}260$ was equal to the number of forest pixels in the study area. For each 23 × 23 m pixel a vector of 24 predictors was available from the remote sensing platforms and other auxiliary sources (Table 1). The response variable was GSV ($m^3\,ha^{-1}$) measured in the field for $n = 1350$ INFC plots and an independent validation set of $n = 332$ plots measured for forest management purposes and for the BIOSOIL project.

We tested four imputation approaches for predicting GSV. Two are non-parametric, random forests and k-NN, and two are parametric, multiple linear regression model and geographically weighted regression model. We optimized the four methods using a leave-one-out (LOO) procedure based on the 1350 NFI plots, with the most accurate approach used to predict GSV for all 40,317,260 forest pixels, hereafter characterized as estimation of the GSV map. Predictions were compared to data for the 332 plots of the independent validation set and were used for small-scale aggregated estimation with a model-assisted approach.

In the next sections, we present details for:

(i) the different imputation approaches for predicting GSV and how we optimized these methods with a LOO cross validation technique;
(ii) estimation of the GSV map applying the most accurate approach formerly identified and assessment of its accuracy using the independent validation set;
(iii) small-scale GSV estimation at study area, region (NUT-2) and province (NUT-3) levels.

3.1. Modelling methods and prediction of growing stock volume

3.1.1. Random forests

Random forests (RF) is a decision tree algorithm and nowadays is among the most popular ensemble methods for classifying and predicting forest variables. The algorithm was introduced by Breiman (1996), and its application for the spatial prediction of forest variables using remotely sensed data is well-documented (Baccini et al., 2012; Evans and Cushman, 2009; Falkowski et al., 2009; Houghton, 2007; Stumpf and Kerle, 2011; Yu et al., 2011). RF generates a set of regression trees (n_{tree}) that are aggregated to produce predictions without overfitting the data (Breiman, 2001). To build and grow trees, RF uses a randomly chosen subset of predictors at each splitting node (m_{try}), and trees are grown without the need of pruning. To grow trees, RF uses a procedure called out-of-bag samples (OOB) where each tree is built independently to arrive at the maximum size based on bootstrap samples from the training dataset (i.e., two-thirds of the data), while the remaining one-third of the sample are randomly left out. The OOB allow calculation of an OOB error rate and variable importance measured by calculating the percent increase in the mean square error when the OOB data for each variable are permuted (Breiman, 2001). The predictors that produce the most accurate splits are chosen from a random subset (m_{try}) of the entire predictor set (p).

Following the OOB sample procedure, the prediction error (OBB error) for each of the individual trees can be estimated as:

$$OOB_{error} = \frac{1}{n}\sum_{i=1}^{n}(y_i - \hat{y}_i)^2 \quad (1)$$

where $\hat{y}_i$ is the predicted output of an OOB sample and y_i is the actual output and n is the total number of OOB sample units.

Among the 24 predictors variables (Table 1), RF was optimized for the number of predictors, n_{tree} and m_{try}. We optimized the number of predictor variables (p) to eliminate irrelevant variables. The cross validation error rate (CV_e) was calculated to assess the performance of each value of p adopted in the model with predictors being removed at each step using various m_{try} functions ($m_{try} = p, p/2, p/3, p/5, p/6 \ldots. p/n$) using the same procedure described by Li et al. (2017).

RF was optimized by searching for the combination of n_{tree} and m_{try} that minimized the OOB error. More details on RF imputation can be found in the review of Belgiu and Drăgu (2016) and in the research article of Li et al. (2017). All analyses in this study were performed using the *randomForest* package within the statistical software package R 3.2.0 (Liaw and Wiener, 2002) (https://www.r-project.org).

3.1.2. k-Nearest neighbors

With the k-Nearest Neighbors (k-NN) technique, predictions are calculated as linear combinations of observations for sample units that are nearest to population units for which predictions are desired with respect to a selected distance metric in a space of feature (auxiliary) variables. Chirici et al. (2016) provided a detailed description of the k-NN method and documented more than 250 k-NN forestry applications based on remote sensing for more than 25 countries on six continents. Optimization included consideration of all possible combination of feature variables and selection of the subset that minimized RMSE. For the selected feature variables, we adopted an equal weighting approach. Simultaneously with the selection of feature variables, we searched for *i)* the optimal number of nearest neighbors, k, used for prediction between a minimum of $k = 1$ and a maximum of $k = 40$; and *ii)* the optimal distance metric among unweighted Euclidean, weighted Euclidean, and Canonical Correlation Analysis (CCA) (McRoberts et al., 2016a,b).

3.1.3. Multiple linear regression

Multiple linear regression (MLR) techniques entail the use of models of the form:

$$y_i = \beta_0 + \beta_1 \bullet x_{1i} + \bullet\bullet\bullet + \beta_p \bullet x_{pi} + \varepsilon_i \quad (2)$$

where i indexes sample units, y_i denotes the single response variable, $p \geq 1$ denotes the number of predictor variables, $j = 1, \ldots, p$ indexes the predictor variables, $\beta\ j$ is the respective regression coefficient, and ε_i denotes a random residual term assumed to be distributed $N(0, \sigma_i^2)$. The model was optimized by comparing all possible combinations of all numbers of predictors with coefficients estimated using ordinary least square. Negative GSV predictions were set to 0, and the cross-validation accuracy assessment was performed after this transformation.

3.1.4. Geographically weighted regression

Geographically Weighted Regression (GWR) is a variant of locally weighted regression, which was originally developed by Cleveland and Devlin, 1998, proposed for geographical applications by Brunsdon et al. (1996), and introduced into the remote sensing community by Maselli (2002). Mathematically, GWR entails constructing a linear regression model for each target unit by weighting the values of the reference units according to the Euclidean (geographic) distance between the target unit and the reference units used for prediction. GWR can, therefore, be easily used for forest inventory applications where reference units (plot) are regularly distributed in geographical space (Maselli, 2002).

Using the same notation as for multiple linear regression, the GWR model can be written in the form:

$$y_i = \beta_0^* + \beta_1^* \bullet x_{1i} + \bullet\bullet\bullet + \beta_p^* \bullet x_{pi} + \varepsilon_i \quad (3)$$

where β^* are the geographically weighted regression coefficients, which are estimated for each target unit from relevant statistics (mean vectors and variance-covariance matrices) computed by giving different weights to the N reference units.

A fundamental step for the application of GWR is therefore the

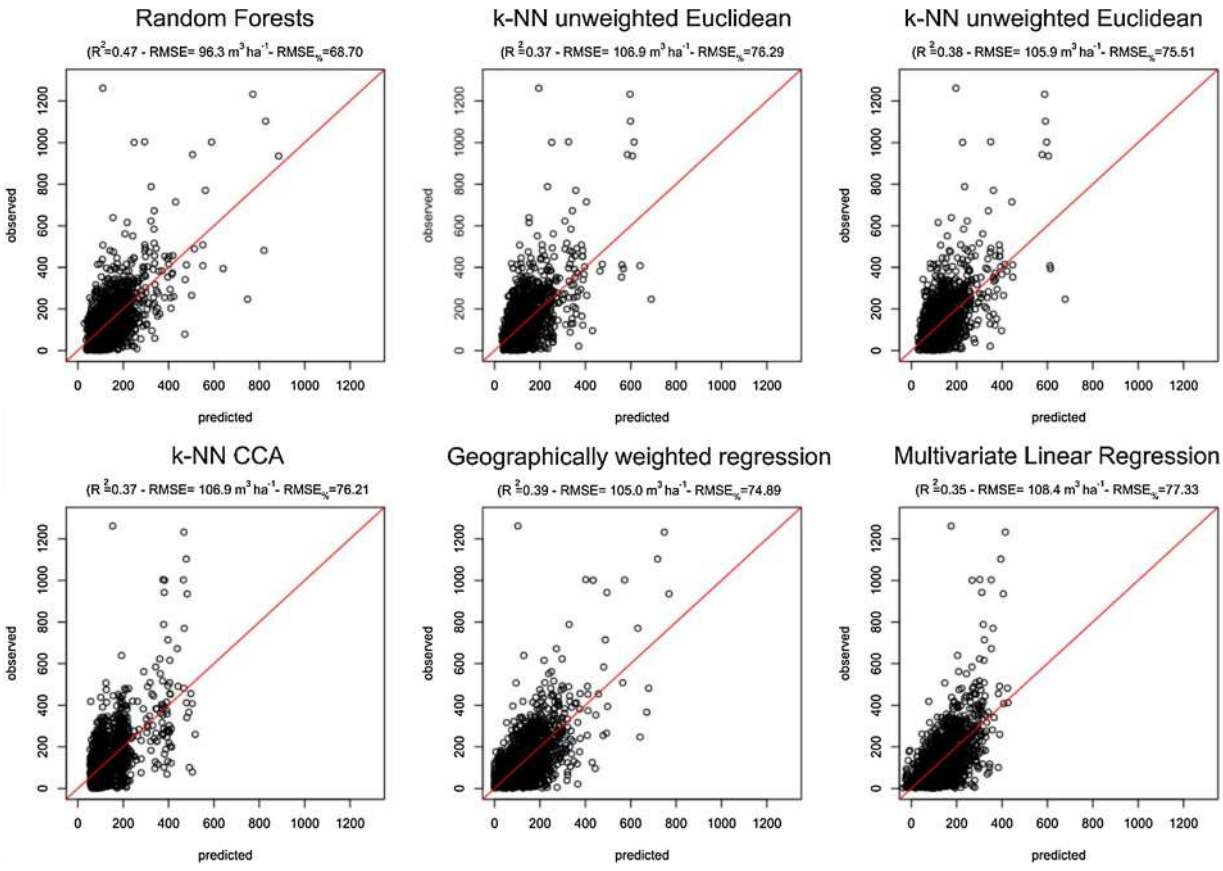

Fig. 4. Scatterplots of GSV observations versus predictions for all the imputation approaches. R^2, RMSE and $RMSE_{\%}$ are based on LOO cross-validation during the optimization phase.

definition of a suitable function to compute these weights. An efficient option is given by a negative exponential function of the spatial Euclidean Distance (ED), i.e. $exp^{(-ED/EDR)}$, which is regulated by the distance range (EDR). The model was optimized as in 3.1.3 using a LOO cross validation strategy, which also served to identify the optimum EDR (see Maselli, 2002, for details).

3.2. Model optimization

During the optimization phase the performance of the different configurations of the four imputation methods was evaluated using the LOO cross validation technique. Each reference set unit is deleted in sequence and predicted using the remaining reference set units (McRoberts et al., 2015).

For each method, we calculated the coefficient of determination (R^2) between the measured and predicted values, the root main square error (RMSE), and the relative RMSE ($RMSE_{\%}$). The RMSE was calculated as:

$$RMSE = \sqrt{\frac{\sum_{i=1}^{n}(y_i - \hat{y}_i)^2}{n}} \quad (4)$$

where n is equal to 1350 (the number of field plots), y_i is the value of the GSV observed in the field, and $\hat{y}_i$ is the predicted value of the GSV. $RMSE_{\%}$ was calculated as the percent of RMSE against the mean value of the GSV observations in the 1350 NFI plots. The optimization was finalized by selecting the most accurate method based on RMSE for the estimation phase.

3.3. Mapping and small-scale estimation

The most accurate imputation approach was used to construct a regular 23 m resolution GSV map.

We assessed the accuracy of the GSV map by comparing map unit estimates and field observations for the independent validation set of 332 plots. Again, following the same approach used in the optimization phase described in § 3.2, we estimated the coefficient of determination (R^2), the root mean square error (RMSE) and the relative RMSE ($RMSE_{\%}$). RMSE was calculated as reported in Eq. 4, where n this time is equal to 332.

To construct an inference for the mean value of the GSV for the whole study area, the model-assisted, generalized regression estimators were used (Särndal et al., 1992; Särndal et al., 2003; Breidt and Opsomer, 2009; McRoberts et al., 2016a,b). Before doing so we deleted from the GSV map all the non-forest pixels on the basis of the forest mask (§ 2.4.3).

The map-based estimate of the mean GSV in the forest area was:

$$\hat{\mu}_{map} = \frac{1}{N}\sum_{j=1}^{N}\hat{y}_i \quad (5)$$

where N was the number of 23 m x 23 m forested population units in the study area and $\hat{y}_i$ is the model prediction for the *i-th* population or map unit. However, the map-based estimate must be adjusted for systematic prediction errors using a bias estimate calculated as:

$$\hat{Bias}(\hat{\mu}_{map}) = \frac{1}{n}\sum_{i=1}^{n}(\hat{y}_i - y_i) \quad (6)$$

where n is the sample size of INFC (i.e. 1350 plots), $\hat{y}_i$ is the model prediction for the *i-th* sample INFC plot and y_i is the observed value for the *i-th* INFC plot. The model-assisted estimate is the map estimate with the estimated bias subtracted:

$$\hat{\mu}_{model-assisted} = \hat{\mu}_{map} - \hat{Bias}(\hat{\mu}_{map}) \quad (7)$$

while the standard error (SE) of $\hat{\mu}_{model-assisted}$ is:

$$SE\ (\hat{\mu}_{model-assisted}) = \sqrt{V\hat{a}r(\hat{\mu}_{model-assisted})} = \sqrt{\frac{1}{n(n-1)}\sum_{i=1}^{n}(e_i - \bar{e})^2} \quad (8)$$

where $e_i = (\hat{y}_i - y_i)$ and $\bar{e} = \frac{1}{n}\sum_{i=1}^{n} e_i$

In addition, to assess the efficiency of the model-assisted estimator we compared it with the original design-based estimates produced by the INFC and its relative efficiency coefficient (RE) calculated as:

$$RE = \frac{V\hat{a}r(\hat{\mu}_{NFI})}{V\hat{a}r(\hat{\mu}_{model-assisted})} \quad (9)$$

Because RE coefficient is the ratio between the variances of $V\hat{a}r(\hat{\mu}_{NFI})$ and $V\hat{a}r(\hat{\mu}_{model-assisted})$, values greater than 1 are evidence of greater precision in the model-assisted estimates (Moser et al., 2017). RE coefficient can be interpreted as the factor by which the original sample size would have to be increased to achieve the same precision as that achieved using the remotely sensed auxiliary data.

4. Results

4.1. Optimization

All the four imputation methods produced comparable results with only limited differences. Independently of the parameter used for evaluating the results, RF always achieved the greatest accuracy and MLR the least accuracy. R^2 ranged between 0.35 and 0.47; RMSE between 96.3 $m^3\,ha^{-1}$ and 108.42 $m^3\,ha^{-1}$; and $RMSE_{\%}$ between 68.70% and 77.3% (Fig. 4)

The three different k-NN configurations achieved very similar results with R^2 ranging between 0.369 and 0.382, RMSE ranging between 105.86 $m^3\,ha^{-1}$ and 106.96 $m^3\,ha^{-1}$, and $RMSE_{\%}$ ranging between 75.51% and 76.29% with $k = 21$ for the Euclidean methods and $k = 54$ for the CCA approach.

For the GWR approach we found an optimal EDR of 0.107° with performances very similar to those achieved for k-NN with R^2 of 0.396, RMSE of 105.0 $m^3\,ha^{-1}$ and $RMSE_{\%}$ of 74.89, and always more accurate than MLR.

Of the 24 available predictors considered during the optimization phase, only 15 variables were ever selected with nine predictors never selected. In terms of usefulness of the predictors, the variables derived from Landsat images were the most frequently selected; band 5 was the only one selected by all six models, followed by band 3 selected by five models. The HV polarization of radar backscattering was selected by four models, the rest of the Landsat bands were selected by three models with the exception of band 4 that was selected for two models; similar results were found for HH polarization of radar, precipitation and AWC of top soil. The other variables that were selected at least once were the average annual temperature, the maximum annual temperature, vegetation height, and the volume of rocks in the soil. In terms of number of predictors, k-NN with weighted Euclidean distance metric, k-NN with the unweighted Euclidean distance metric, and GWR all selected five; RF selected six; k-NN with the CCA distance metric selected seven, and MLR selected 10 (Table 2). The full list of the optimization results is reported in Table 2.

Considering these results RF based on six predictors and 300 regression trees was selected for the following estimation phase.

4.2. Estimation

The RF model was used to predict GSV for each of the 4,031,726 23 m x 23 m resolution forest target units in the study area (Fig. 6). GSV predictions ranged between 0 and 1021.54 $m^3\,ha^{-1}$ with a standard deviation of 70.32 $m^3\,ha^{-1}$. For each of the 332 plots in the independent validation set, we predicted GSV using RF and compared it with field observations. We found $R^2 = 0.68$ and RMSE% = 38.2%

Table 2
Parameters used for the different imputation approaches and results reported in terms of R2, RMSE, RMSE%.

Imputation	Type of imputation	Selected predictors	Optimization parameters	R^2	RMSE $m^3\,ha^{-1}$	$RMSE_{\%}$
Random Forests	Non Parametric	LANDSAT_B1 LANDSAT_B3 LANDSAT_B5 LANDSAT_B7 prec SAR_HV CHM	$n_{tree} = 300$	0.47	96.3	68.70
k-NN unweighted based on Euclidean distance	Non Parametric	LANDSAT_B1 LANDSAT_B3 LANDSAT_B5 LANDSAT_B6 AWC_TOP_P	k = 21	0.369	106.96	76.29
k-NN weighted Euclidean based on Euclidean distance	Non Parametric	LANDSAT_B1 LANDSAT_B3 LANDSAT_B5 LANDSAT_B6 AWC_TOP_P	k = 21	0.382	105.86	75.51
k-NN CCA	Non Parametric	LANDSAT_B2 LANDSAT_B4 LANDSAT_B5 LANDSAT_B7 SAR_HV SAR_HHtemp_mean	k = 54	0.370	106.88	76.23
Geographically weighted regression	Parametric	LANDSAT_B2 LANDSAT_B3 LANDSAT_B5 SAR_HV prec	Euclidean distance range (EDR) 0.107°	0.396	105.0	74.89
Multiple Linear Regression	Parametric	LANDSAT_B2 LANDSAT_B3 LANDSAT_B4 LANDSAT_B5 LANDSAT_B6 LANDSAT_B7 SAR_HV SAR_HH temp_mean VS_P		0.352	108.42	77.33

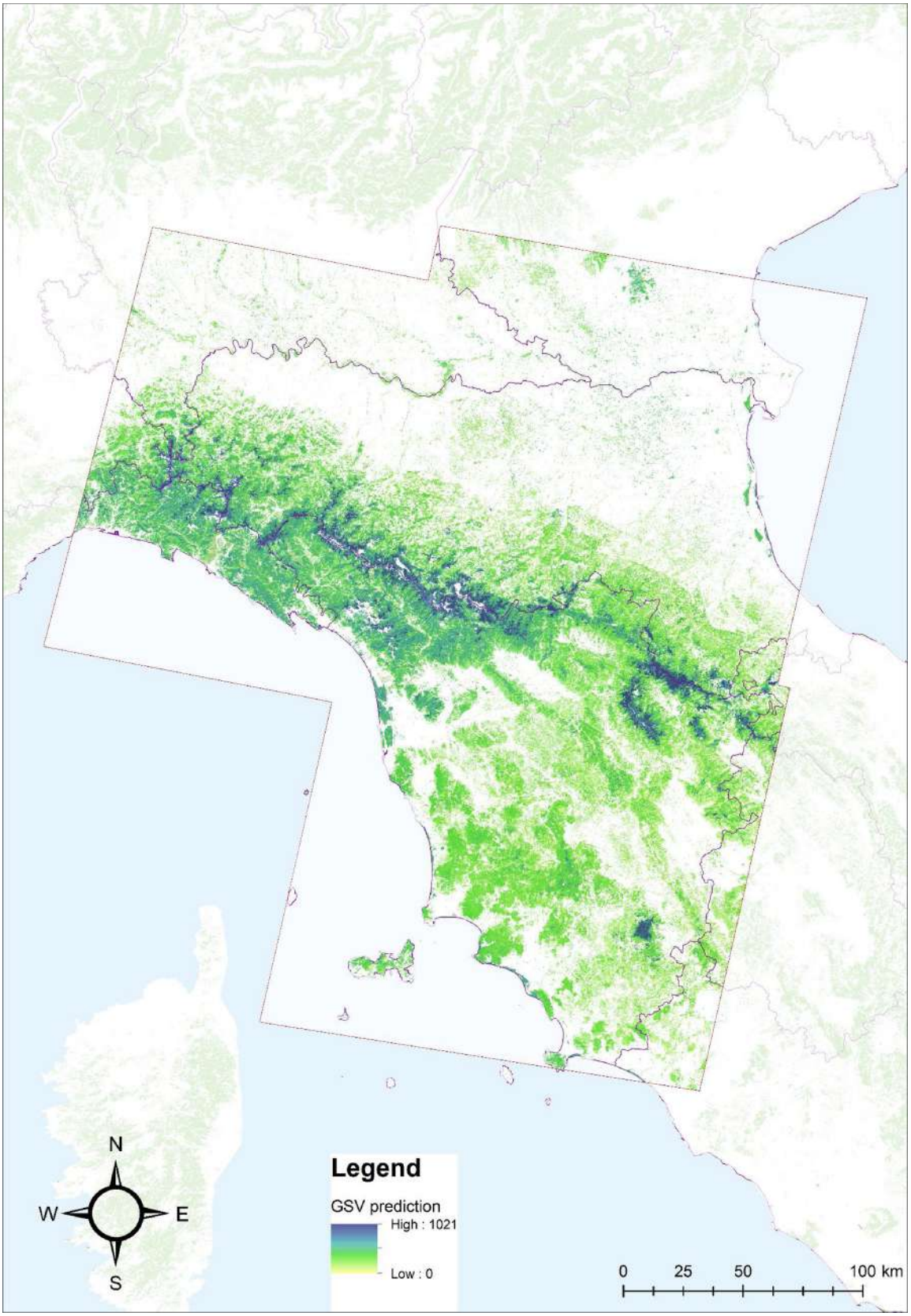

Fig. 5. Growing stock map of the study area generated with Random Forest Imputation. GSV in $m^3\,ha^{-1}$.

(Fig. 5) demonstrating a performance that was greater than achieved using LOO cross-validation.

On the basis of RF estimation for the entire study area, $\hat{\mu}_{model-assisted} = 126.17\ m^3\,ha^{-1}$ with $SE(\hat{\mu}_{model-assisted}) = 2.78\ m^3\,ha^{-1}$, while at regional level $\hat{\mu}_{model-assisted} = 131.58\ m^3\,ha^{-1}$ with $SE(\hat{\mu}_{model-assisted}) = 4.19\ m^3\,ha^{-1}$ for Tuscany, and $\hat{\mu}_{model-assisted}$ $135.42\ m^3\,ha^{-1}$ with $SE(\hat{\mu}_{GREG}) = 5.55\ m^3\,ha^{-1}$ for Emilia Romagna. These regional model-assisted estimates are in line with the official design-based estimates from INFC plots (Gasparini and Tabacchi, 2011; INFC, 2008) which are $128.8\ m^3\,ha^{-1}$ with SE = $4.6\ m^3\,ha^{-1}$ for Tuscany and 128.4 with SE = $7.12\ m^3\,ha^{-1}$ for Emilia-Romagna. These results revealed a RE of 1.09 for Tuscany Region and a RE of 1.28 for Emilia-Romagna Region.

Moreover, the model-assisted estimate of GSV was calculated at province administrative level (Annex 1). Such estimates are not provided by official NFI aggregated statistics.

5. Discussion

The study focused on three objectives: *(i)* to demonstrate that even in large complex Mediterranean landscapes, without the availability of ALS, it is possible to produce spatial wall-to-wall estimates of GSV measured in the field in the National Forest Inventory (INFC, 2004) on the basis of predictors from remotely sensed images and other auxiliary variables, (*ii*) to understand the relative importance of possible predictors available wall-to-wall in Italy and the performance of the different estimation approaches, and *(iii)* to suggest a methodology that can be applied at country level in Italy to produce wall-to-wall predictions of forest variables to support forest planning and management.

To achieve these results for a large study area of $45{,}438\ km^2$ in central Italy, we acquired 24 potential predictors which are available wall-to-wall in Italy and that may directly or indirectly be related to forest biomass and GSV. We compared six different prediction techniques, all of which comparable accuracies but with RF producing the greatest accuracy.

Among the other imputation approaches, GWR yielded the greatest accuracy, in particular outperforming conventional multiple regression. This can be explained considering that the relationships between GSV and virtually all predictors currently considered are affected by several factors which can vary spatially (Lu, 2006). GWR can account for this spatial variability by allowing the per-pixel computation of different regression models. This is particularly relevant in heterogeneous Mediterranean environments, where GWR has already been proficiently applied to Landsat TM/ETM + imagery for forest GSV prediction (Maselli and Chiesi, 2006; Maselli et al., 2014a, b).

Landsat bands of which B5 acquired in short-wave infrared between 1.55 and 1.75 μm was most important, and climate variables of which precipitation was most important, emerged as the most influential predictors. The resulting 23 m resolution GSV map, when compared against an independent set of field measures, demonstrated a good relationship between observed and predicted values ($R^2 = 0.69$ and $RMSE_{\%} = 37.2\%$). However our results are less accurate than those obtained in boreal forests using ALS in Sweden by Nilsson et al. (2017) and in the review of Næsset et al. (2004) for which RMSE usually ranged between 15% and 25% of the average real value measured in the field.

The relatively larger $RMSE_{\%}$ we obtained can be due to several reasons.

Firstly, we did not used metrics from ALS data which are usually the best candidate predictors for GSV estimation. This is confirmed if we compare our results with results reported for studies where ALS was not used. For example Reese et al. (2002), using Landsat data in Sweden, reported pixel-level $RMSE_{\%}$ in the range of 59% and 80%, and Immitzer et al. (2016) in Germany using WorldView-2 imagery report a $RMSE_{\%}$ between 46% and 37%.

Secondly, GSV is relatively small for our forests, we observed a field GSV average of $139\ m^3\,ha^{-1}$, less than half of the $287\ m^3\,ha^{-1}$ reported by Nilsson et al. (2017) in Sweden.

Thirdly, Italy has a heterogeneous landscape, and Mediterranean forests are characterized by considerable complexity in tree species composition and structure relative to temperate and boreal forests.

Moreover, we found that the accuracy of the pixel-level estimation evaluated with the independent dataset was greater than those we found with the LOO procedure in the optimization phase. The result was not expected but it is probably due to the fact that the GSV measured in the independent validation dataset has a more normal distribution around the mean values (Fig. 5) than those from the INFC (Fig. 2) and that the average GSV in the independent validation dataset is also greater ($351\ m^3\,ha^{-1}$) than those measured in INFC plots ($140\ m^3\,ha^{-1}$).

In line with previous results from the literature, we observed an underestimation for large GSV observations, independently of the prediction approach. This effect has anyhow a limited impact when the comparison was done with LOO against the INFC plots because just a few of them have very large GSV observations (Fig. 4). This saturation effect with under-predictions for plots with GSV greater than $600\ m^3\,ha^{-1}$ was well-known because spectral reflectance values are not sensitive, for example, to multilayer canopy forest or dense forests (Zhao et al., 2016). Moreover, some authors have reported that areas characterized by very complex topographic features (i.e. from flat terrain to mountains up to 2000 m a.s.l.) affect the spectral signature and the data saturation values of forest aboveground biomass and growing stock volume (Lu et al., 2012, 2016; Foody et al., 2003; Nichol and Sarker, 2011). However, the saturation effect was reported in the literature even when ALS data were used (Nilsson et al., 2017; Giannetti et al., 2018a,2018b; Lefsky et al., 2005).

Even if RF was found to be the most accurate method, only small differences in prediction accuracies were found across the different non-parametric and parametric methods. Nilsson et al. (2017) reported similar conclusions for Sweden using ALS data.

Regarding the model-assisted estimates calculated on the basis of the GSV map, with the use of our approach it was possible to increase the precision of INFC predictions at regional level (RE = 1.09 in Tuscany and RE = 1.28 in Emilia Romagna) and to provide for the first time growing stock estimates at Province level.

It is important to remember that the use of pixel level estimates of map products similar to those we presented in Fig. 6 is discouraged since GSV predictions in single pixels may be affected by a consistent bias (McRoberts and Tomppo, 2007). We therefore suggest aggregation of predictions from several pixels (Areas Of Interests – AOI), since in case the pixel prediction errors are independent and distributed with zero mean, then when the AOI increases, then averaged value of the pixels tend to equal the real value (McRoberts and Tomppo, 2007). Users could aggregate GSV pixel level estimates to create estimates for different AOIs, for example related to ecological regions, municipality boundaries, or forest management units.

6. Conclusions

Forest tree monitoring and assessment are rapidly evolving as new information needs arise and new techniques and tools become available. However, the exploitation of the latter, as well as their implementation within operative management processes, should be evidence-based (Corona, 2018).

Under this perspective, several conclusions can be drawn from the study. Firstly, Landsat data are confirmed as a reliable and efficient source of information for modeling GSV, even in large and complex Mediterranean forest areas. Secondly, we found that in the Mediterranean area, predictors derived from climate data are a valid spatial data source for modeling GSV most probably because they can describe different growing season conditions. Thirdly, all the tested modelling approaches have the capability to predict GSV with

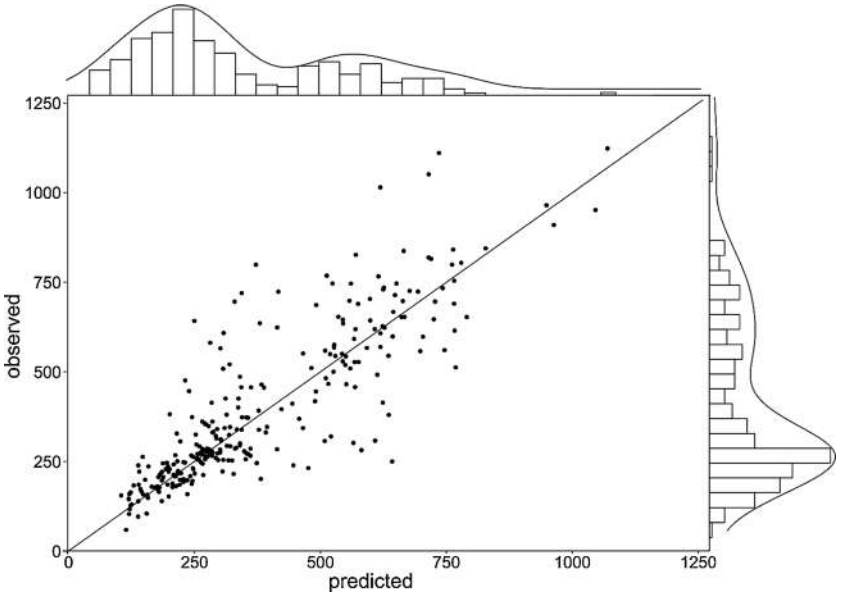

Fig. 6. Scatterplot of GSV observations versus predictions obtained by RF for the 332 units of the independent dataset.

comparable results. Fourthly, the GSV map is confirmed as a valid tool for model-assisted inference at regional and province levels.

We can affirm that the 23 m resolution GSV map we produced can be useful and practical to support the requirements of national and regional forest bodies, forest companies and forest owners. This map could be the basis for decision support systems as proposed by Puletti et al. (2017) for a test area in south Italy, as a tool to assess wood production and harvesting activities in forest proprieties, thereby contributing to improving the Mediterranean forest economy and, if used at forest management scale, reducing the cost for data acquisition needed for the implementation of management plans.

Moreover, the GSV map can be used to produce model-assisted estimates at province level (NUT-3), augmenting the spatial resolution of traditional NFI design-based estimates which are currently available only for administrative Regions (NUT-2) and thus adding value to the INFC. Under this point of view the proposed methodology is now ready for a wall-to-wall application in Italy to move the traditional NFI program to a more modern EFI, in line with achievements in other countries.

Under this point of view it is also strongly recommended that in the future the Italian NFI could evolve in a permanent monitoring system, where a sample of the total number of field plots is visited in the field every year in order to complete the revisit of all the plots in 5–10 years.

In the future we hope that ALS will be finally available wall-to-wall in Italy to facilitate prediction of forest variables estimates with even greater accuracy. In such a context satellite LiDAR data from the Global Ecosystem Dynamics Investigations (GEDI space laser data) and from the ICESAT-2 (Geoscience Laser Altimeter System - GLAS) are potentially extremely important in Italy if ALS will not be available sooner.

Appendix A

Small-scale estimates of mean GSV ($m^3\,ha^{-1}$) obtained with RF model at Province (NUT-3) level. For each Province we also report the forest area estimation from the second Italian National Forest Inventory (INFC, 2007, 2008; Gasparini and Tabacchi, 2011).

Region	Province	Province Area (km^2)	Total Forest Area (km^2) (INFC)	SE Total Forest Area (%) (INFC)	n_i	GSV $\hat{\mu}_{GREG}(m^3\,ha^{-1})$	GSV $SE(\hat{\mu}_{GREG})(\%)$
Tuscany	Arezzo	323300	1792,19	4.2	127	111.13	8.5
	Firenze	351369	1785,00	4.2	117	151.89	12.3
	Grosseto	450312	1979,61	4.0	116	98.35	8.6
	Livorno	121371	473,64	8.6	23	108.88	16.7
	Lucca	177322	1210,44	5.2	64	198.86	13.1
	Massa Carrara	115468	867,13	6.2	30	148.69	14.69
	Pisa	244472	950,53	6.0	54	98.82	11.28
	Pistoia	96412	506,40	8.3	32	214.30	43.91
	Prato	36572	233,34	12.3	13	186.87	24.1
	Siena	38298	1717,10	4.3	115	85.81	6.09
Emilia-Romagna	Bologna	370232	1007,61	5.6	56	112.60	11.12
	Forlì-Cesena	237840	1066,21	5.5	70	86.08	15.24
	Modena	268802	686,95	7.0	49	123.97	14.97
	Parma	344748	1525,42	4.4	85	170.81	9.94
	Piacenza	258586	848,37	6.2	51	111.66	13.07
	Ravenna	185944	213,32	13.0	19	80.55	12.39
	Reggio Emilia	229126	635,18	7.3	58	126.75	11.26
Liguria	La Spezia	88135	542,29	7.6	46	144.55	16.34

References

Baccini, A., Goetz, S.J., Walker, W.S., Laporte, N.T., Sun, M., Sulla-Menashe, D., Hackler, J., Beck, P.S.A., Dubayah, R., Friedl, M.A., Samanta, S., Houghton, R.A., 2012. Estimated carbon dioxide emissions from tropical deforestation improved by carbon-density maps. Nat. Clim. Chang. 2, 182.

Barbati, A., Marchetti, M., Chirici, G., Corona, P., 2014. European Forest Types and Forest Europe SFM indicators: tools for monitoring progress on forest biodiversity conservation. For. Ecol. Manage. 321, 145–157. https://doi.org/10.1016/j.foreco.2013.07.004.

Barrett, F., McRoberts, R.E., Tomppo, E., Cienciala, E., Waser, L.T., 2016. A questionnaire-based review of the operational use of remotely sensed data by national forest inventories. Remote Sens. Environ. 174, 279–289. https://doi.org/10.1016/j.rse.2015.08.029.

Belgiu, M., Drăgu, L., 2016. Random forest in remote sensing: a review of applications and future directions. ISPRS J. Photogramm. Remote. Sens. 114, 24–31. https://doi.org/10.1016/j.isprsjprs.2016.01.011.

Borghetti, M., Chirici, G., 2016. Raw data from the Italian National Forest Inventory are on-line and publicly available. For. - Riv. Di Selvic. Ed Ecol. For. 13, 33–34. https://doi.org/10.3832/efor0083-013.

Bottalico, F., Chirici, G., Giannini, R., Mele, S., Mura, M., Puxeddu, M., McRoberts, R.E., Valbuena, R., Travaglini, D., 2017. Modeling Mediterranean forest structure using airborne laser scanning data. Int. J. Appl. Earth Obs. Geoinf. 57, 145–153. https://doi.org/10.1016/j.jag.2016.12.013.

Boudreau, J., Nelson, R.F., Margolis, H.A., Beaudoin, A., Guindon, L., Kimes, D.S., 2008. Regional aboveground forest biomass using airborne and spaceborne LiDAR in Québec. Remote Sens. Environ. 112, 3876–3890. https://doi.org/10.1016/j.rse.2008.06.003.

Breidenbach, J., Astrup, R., 2012. Small area estimation of forest attributes in the Norwegian National Forest Inventory. Eur. J. For. Res. 131, 1255–1267. https://doi.org/10.1007/s10342-012-0596-7.

Breidt, F.J., Opsomer, J.D., 2009. . Chapter 27 - nonparametric and semiparametric estimation in complex surveys. In: Rao, C.R. (Ed.), Handbook of Statistics, Handbook of Statistics. Elsevier, pp. 103–119. https://doi.org/10.1016/S0169-7161(09)00227-2.

Breiman, L., 2001. Random forests. Mach. Learn. 45, 5–32. https://doi.org/10.1023/A:1010933404324.

Breiman, L., 1996. Bagging predictors. Mach. Learn. 24, 123–140. https://doi.org/10.1023/A:1018054314350.

Brosofske, K.D., Froese, R.E., Falkowski, M.J., Banskota, A., 2014. A review of methods for mapping and prediction of inventory attributes for operational forest management. For. Sci. 60, 733–756. https://doi.org/10.5849/forsci.12-134.

Brunsdon, C., Fotheringham, A.S., Charlton, M.E., 1996. Geographically weighted regression: a method for exploring spatial nonstationarity. Geogr. Anal. 28, 281–298.

Chirici, G., 2019. A preliminary comparison between IMAGE2006 and landsat 5 TM imagery for the wall-to-wall spatial estimation of growing stock volume in Italy (in press). Proceedings of the 11TH Session of the Winter Forest School at the Forest Research Institute „Application of Geoinformatics in Forestry" 12-14 March.

Chirici, G., McRoberts, R.E., Winter, S., Bertini, R., Bröändli, U.-B., Asensio, I.A., Bastrup-Birk, A., Rondeux, J., Barsoum, N., Marchetti, M., 2012. National forest inventory contributions to forest biodiversity monitoring. For. Sci. 58, 257–268. https://doi.org/10.5849/forsci.12-003.

Chirici, G., Mura, M., McInerney, D., Py, N., Tomppo, E.O., Waser, L.T., Travaglini, D., McRoberts, R.E., 2016. A meta-analysis and review of the literature on the k-Nearest Neighbors technique for forestry applications that use remotely sensed data. Remote Sens. Environ. 176, 282–294. https://doi.org/10.1016/j.rse.2016.02.001.

Cleveland, W.S., Devlin, S.J., 1998. Locally weighted regression: an approach to regression analysis by local fitting. J. Comput. Graph. Stat. 83, 596–610.

Condés, S., McRoberts, R.E., 2017. Updating national forest inventory estimates of growing stock volume using hybrid inference. For. Ecol. Manage. 400, 48–57.

Corona, P., 2010. Integration of forest mapping and inventory to support forest management. IForest 3, 59–64. https://doi.org/10.3832/ifor0531-003.

Corona, P., 2018. Communicating facts, findings and thinking to support evidence-based strategies and decisions. Ann. Silvicult. Res. 42, 1–2. https://doi.org/10.12899/asr-1617.

Corona, P., Chirici, G., McRoberts, R.E., Winter, S., Barbati, A., 2011. Contribution of large-scale forest inventories to biodiversity assessment and monitoring. For. Ecol. Manage. 262, 2061–2069. https://doi.org/10.1016/j.foreco.2011.08.044.

Corona, P., Fattorini, L., Franceschi, S., Chirici, G., Maselli, F., Secondi, L., 2014. Mapping by spatial predictors exploiting remotely sensed and ground data: a comparative design-based perspective. Remote Sens. Environ. 152, 29–37. https://doi.org/10.1016/j.rse.2014.05.011.

Evans, J.S., Cushman, S.A., 2009. Gradient modeling of conifer species using random forests. Landsc. Ecol. 24, 673–683. https://doi.org/10.1007/s10980-009-9341-0.

Falkowski, M.J., Evans, J.S., Martinuzzi, S., Gessler, P.E., Hudak, A.T., 2009. Characterizing forest succession with lidar data: an evaluation for the Inland Northwest, USA. Remote Sens. Environ. 113, 946–956. https://doi.org/10.1016/j.rse.2009.01.003.

FAO, 2013. Strategic Framework on Mediterranean Forests. High Level Segment of the Third Mediterranean Forest Week, Tlemcen March 21, 2013.

FAO, 2010. Global Forest Resources Assessment 2010. FAO Forestry Paper 163, 350 pp. doi:ISBN 978-92-5-106654-6.

FAO, F. and A.O., UNCCD, G.M. of the, 2015. Sustainable Financing for Forest and Landscape Restoration: the Role of Public Policy Makers. pp. 12.

Fattorini, L., Marcheselli, M., Pisani, C., 2006. A three-phase sampling strategy for large-scale multiresource forest inventories. J. Agric. Biol. Environ. Stat. 11, 296–316. https://doi.org/10.1198/108571106X130548.

Fernández-Landa, A., Fernández-Moya, J., Tomé, J.L., Algeet-Abarquero, N., Guillén-Climent, M.L., Vallejo, R., Sandoval, V., Marchamalo, M., 2018. High resolution forest inventory of pure and mixed stands at regional level combining National Forest Inventory field plots, Landsat, and low density lidar. Int. J. Remote Sens. 0, 1–15. https://doi.org/10.1080/01431161.2018.1430406.

Fibbi, L., Chiesi, M., Moriondo, M., Bindi, M., Chirici, G., Papale, D., Maselli, M., 2016. Correction of a 1 km daily rainfall dataset for modelling forest ecosystem processes in Italy. Meteorol. Appl. https://doi.org/10.1002/met.1554.

Foody, G.M., Boyd, D.S., Cutler, M.E.J., 2003. Predictive Relations of Tropical Forest Biomass from Landsat TM Data and Their Transferability between Regions 85. pp. 463–474. https://doi.org/10.1016/S0034-4257(03)00039-7.

FOREST EUROPE, 2015. FOREST EUROPE Liaison Unit MadridState of Europe'S Forests 2015., Ministerial Conference on the Protection of Forests in Europe2015. State of Europe'S Forests 2015., Ministerial Conference on the Protection of Forests in Europe.

Fornaciai, A., Favalli, M., Karátson, D., Tarquini, S., Boschi, E., 2012. Morphometry of scoria cones, and their relation to geodynamic setting: A DEM-based analysis. J. Volcanol. Geotherm. Res. 217–218, 56–72. https://doi.org/10.1016/j.jvolgeores.2011.12.012.

Galluzzi, M., Giannetti, F., Puletti, N., Canullo, R., Rocchini, D., Bastrup, A., Gherardo, B., 2019. A plot level exploratory analysis of European forest based on the results from the BioSoil Forest Biodiversity project. Eur. J. For. Res. https://doi.org/10.1007/s10342-019-01205-2.

L'inventario nazionale delle foreste e dei serbatoi forestali di carbonio INFC 2005. In: Gasparini, P., Tabacchi, G. (Eds.), Secondo Inventario Forestale Nazionale Italiano. Metodi E Risultati. Ministero Delle Politiche Agricole, Alimentari E Forestali; Corpo Forestale Dello Stato. Consiglio Per La Ricerca E La Sperimentazione in Agricoltura, Unità Di Ricerca Per Il Monitoraggio E La Pianificazione Forestale. Edagricole-Il Sole 24 Ore, Bologna, 653 pp.

Giannetti, F., Barbati, A., Mancini, L.D., Travaglini, D., Bastrup-Birk, A., Canullo, R., Nocentini, S., Chirici, G., 2018a. European Forest Types: toward an automated classification. Ann. For. Sci. https://doi.org/10.1007/s13595-017-0674-6.

Giannetti, F., Chirici, G., Gobakken, T., Næsset, E., Travaglini, D., Puliti, S., 2018b. A new approach with DTM-independent metrics for forest growing stock prediction using UAV photogrammetric data. Remote Sens. Environ. 213. https://doi.org/10.1016/j.rse.2018.05.016.

Ginzler, C., Hobi, M., 2015. Countrywide stereo-image matching for updating digital surface models in the framework of the swiss national forest inventory. Remote Sens. 7, 4343–4370. https://doi.org/10.3390/rs70404343.

Haylock, M.R., Hofstra, N., Klein Tank, A.M.G., Klok, E.J., Jones, P.D., New, M., 2008. A European daily high-resolution gridded dataset of surface temperature and precipitation. J. Geophys. Res. Atmos. 113, D20119.

Hobi, M.L., Ginzler, C., 2012. Accuracy assessment of digital surface models based on WorldView-2 and ADS80 stereo remote sensing data. Sensors Basel (Basel) 12, 6347–6368. https://doi.org/10.3390/s120506347.

Hollaus, M., Dorigo, W., Wagner, W., Schadauer, K., Höfle, B., Maier, B., 2009. Operational wide-area stem volume estimation based on airborne laser scanning and national forest inventory data. Int. J. Remote Sens. 30, 5159–5175. https://doi.org/10.1080/01431160903022894.

Houghton, R.A., 2007. Balancing the global carbon budget. Annu. Rev. Earth Planet. Sci. 35, 313–347. https://doi.org/10.1146/annurev.earth.35.031306.140057.

Immitzer, M., Stepper, C., Böck, S., Straub, C., Atzberger, C., 2016. Forest Ecology and Management Use of WorldView-2 stereo imagery and National Forest Inventory data for wall-to-wall mapping of growing stock. For. Ecol. Manage. 359, 232–246. https://doi.org/10.1016/j.foreco.2015.10.018.

INFC, 2008. Le stime di superficie – risultati per macroaree e Province. In: Gasparini, A.P., Di Cosmo, L., Gagliano, C., Tabacchi, G.M.G. (Eds.), Inventario Nazionale delle Foreste e dei Serbatoi Forestali di Carbonio. MiPAAF – Ispettorato Generale Corpo Forestale dello Stato, CRA-MPF, Trento.

INFC, 2007. Le stime di superficie 2005 - seconda parte. In: Tabacchi, A.G., De Natale, F., Di Cosmo, L., Floris, A., Gagliano, C., Gasparini, P., Salvadori, I., Scrinzi, G., Tosi, V. (Eds.), Inventario Nazionale delle Foreste e dei Serbatoi Forestali di Carbonio. MiPAF – Corpo Forestale dello Stato - Ispettorato Generale, CRA - ISAFA, Trento. Available from: http://www.infc.it [on line].

INFC, 2004. Il disegno di campionamento. Inventario Nazionale delle Foreste e dei Serbatoi Forestali di Carbonio. MiPAF - Direzione Generale per le Risorse Forestali Montane e Idriche, Corpo Forestale dello Stato, ISAFA, Trento 36 p. http://www.isafa.it/scientifica/.

Kangas, A., Astrup, R., Breidenbach, J., Fridman, J., Gobakken, T., Korhonen, K.T., Maltamo, M., Nilsson, M., Nord-Larsen, T., Næsset, E., Olsson, H., 2018. Remote sensing and forest inventories in Nordic countries – roadmap for the future. Scand. J. For. Res. 7581, 1–16. https://doi.org/10.1080/02827581.2017.1416666.

Lefsky, M.A., Hudak, A.T., Cohen, W.B., Acker, S.A., 2005. Geographic variability in lidar predictions of forest stand structure in the Pacific Northwest. Remote Sens. Environ. 95, 532–548. https://doi.org/10.1016/j.rse.2005.01.010.

Li, wang, Z., XIN, ping, X., TANG, H., YANG, F., CHEN, B., ZHANG, B., 2017. Estimating grassland LAI using the Random Forests approach and Landsat imagery in the meadow steppe of Hulunber, China. J. Integr. Agric. 16, 286–297. https://doi.org/10.1016/S2095-3119(15)61303-X.

Liaw, A., Wiener, M., 2002. Classification and regression by randomForest. Nucleic Acids Res. 5, 983–999. https://doi.org/10.1023/A:1010933404324.

Lu, D., Chen, Q., Wang, G., Liu, L., Li, G., 2016. A survey of remote sensing-based aboveground biomass estimation methods in forest ecosystems. Int. J. Digit. Earth 0, 1–43. https://doi.org/10.1080/17538947.2014.990526.

Lu, D., Chen, Q., Wang, G., Moran, E., Batistella, M., Zhang, M., Laurin, G.V., Saah, D., 2012. Aboveground Forest Biomass Estimation With Landsat and LiDAR Data and

Uncertainty Analysis of the Estimates. https://doi.org/10.1155/2012/436537.
Lu, D., 2006. The potential and challenge of remote sensing-based biomass estimation. Int. J. Remote Sens. 27 (7), 1297–1328.
Mardia, K.V., Kent, J.T., Bibby, J.M., 1979. Multivariate Analysis. Academic Press ISBN 0-12-471252-5.
Maselli, F., 2002. Improved estimation of environmental parameters through locally calibrated multivariate regression analyses. Photogramm. Eng. Remote Sensing 68, 1163–1171.
Maselli, F., Pasqui, M., Chirici, G., Chiesi, M., Fibbi, L., Salvati, R., Corona, P., 2012. Modeling primary production using a 1 km daily meteorological data set. Clim. Res. 54, 271–285.
Maselli, F., Chiesi, M., Mura, M., Marchetti, M., Corona, P., Chirici, G., 2014a. Combination of optical and LiDAR satellite imagery with forest inventory data to improve wall-to-wall assessment of growing stock in Italy. Int. J. Appl. Earth Observ. Geoinform. 26, 377–386. https://doi.org/10.1016/j.jag.2013.09.001.
Maselli, F., Chiesi, M., 2006. Evaluation of statistical methods to estimate forest volume in a Mediterranean region. IEEE Trans. Geosci. Remote. Sens. 44 (8), 2239–2250.
Maselli, F., Chiesi, M., Corona, P., 2014b. Use of geographically weighted regression to enhance the spatial features of forest attribute maps. J. Appl. Remote Sens. 8 (1), 083533. https://doi.org/10.1117/1.JRS.8.083533.
Matasci, G., Hermosilla, T., Wulder, M.A., White, J.C., Coops, N.C., Hobart, G.W., Zald, H.S.J., 2018. Large-area mapping of Canadian boreal forest cover, height, biomass and other structural attributes using Landsat composites and lidar plots. Remote Sens. Environ. 209, 90–106. https://doi.org/10.1016/j.rse.2017.12.020.
McRoberts, R., Tomppo, E., Schadauer, K., Vidal, C., Stahl, G., Chirici, G., Lanz, A., Cienciala, E., Winter, S., Smith, B., 2009. Harmonizing national forest inventories. J. For. 179–187.
McRoberts, R.E., Cohen, W.B., Næsset, E., Stehman, S.V., Tomppo, E.O., 2010b. Using remotely sensed data to construct and assess forest attribute maps and related spatial products. Scand. J. For. Res. 25, 340–367. https://doi.org/10.1080/02827581.2010.497496.
McRoberts, R.E., Domke, G.M., Chen, Q., Næsset, E., Gobakken, T., 2016a. Using genetic algorithms to optimize k-Nearest Neighbors configurations for use with airborne laser scanning data. Remote Sens. Environ. 184, 387–395. https://doi.org/10.1016/j.rse.2016.07.007.
McRoberts, R.E., Tomppo, E.O., 2007. Remote sensing support for national forest inventories. Remote Sens. Environ. 110, 412–419. https://doi.org/10.1016/j.rse.2006.09.034.
McRoberts, R.E., Tomppo, E.O., Næsset, E., 2010a. Advances and emerging issues in national forest inventories. Scand. J. For. Res. 25, 368–381.
McRoberts, R.E., Næsset, E., Gobakken, T., 2015. Optimizing the k-Nearest Neighbors technique for estimating forest aboveground biomass using airborne laser scanning data. Remote Sens. Environ. 163, 13–22.
McRoberts, R.E., Chen, Q., Domke, G.M., Ståhl, G., Saarela, S., Westfall, J.A., 2016b. Hybrid estimators for mean aboveground carbon per unit area. For. Ecol. Manage. 378, 44–56.
McRoberts, R.E., Chen, Q., Walters, B.F., Kaisershot, D.J., 2018. The effects of global positioning system receiver accuracy on airborne laser scanning-assisted estimates of aboveground biomass. Remote Sens. Environ. 207, 42–49.
Montaghi, A., Corona, P., Dalponte, M., Gianelle, D., Chirici, G., Olsson, H., 2013. Airborne Laser Scanning of Forest Resources: an overview of research in Italy as a commentary case study. Int. J. Appl. Earth Obs. Geoinf. 23, 288–300. https://doi.org/10.1016/j.jag.2012.10.002.
Moser, P., Vibrans, A.C., McRoberts, R.E., Næsset, E., Gobakken, T., Chirici, G., Mura, M., Marchetti, M., 2017. Methods for variable selection in LiDAR-assisted forest inventories. Forestry 90, 112–124. https://doi.org/10.1093/forestry/cpw041.
Mura, M., Bottalico, F., Giannetti, F., Bertani, R., Giannini, R., Mancini, M., Orlandini, S., Travaglini, D., Chirici, G., 2018. Exploiting the capabilities of the Sentinel-2 multi spectral instrument for predicting growing stock volume in forest ecosystems. Int. J. Appl. Earth Obs. Geoinf. 66, 126–134. https://doi.org/10.1016/j.jag.2017.11.013.
Mura, M., McRoberts, R.E., Chirici, G., Marchetti, M., 2015. Estimating and mapping forest structural diversity using airborne laser scanning data. Remote Sens. Environ. 170, 133–142. https://doi.org/10.1016/j.rse.2015.09.016.
Næsset, E., 2007. Airborne laser scanning as a method in operational forest inventory: status of accuracy assessments accomplished in Scandinavia. Scand. J. For. Res. 22 433–422.
Næsset, E., Bollandsås, O.M., Gobakken, T., Gregoire, T.G., Ståhl, G., 2013. Model-assisted estimation of change in forest biomass over an 11year period in a sample survey supported by airborne LiDAR: a case study with post-stratification to provide "activity data.". Remote Sens. Environ. 128, 299–314. https://doi.org/10.1016/j.rse.2012.10.008.
Næsset, E., Gobakken, T., Holmgren, J., Hyyppä, H., Hyyppä, J., Maltamo, M., Nilsson, M., Olsson, H., Persson, Å., Söderman, U., 2004. Laser scanning of forest resources: the nordic experience. Scand. J. For. Res. 19, 482–499. https://doi.org/10.1080/02827580410019553.
Nichol, J.E., Sarker, L.R., 2011. Improved biomass estimation using the texture parameters of two high-resolution. Optical Sensors 49, 930–948.
Nilsson, M., Nordkvist, K., Jonzén, J., Lindgren, N., Axensten, P., Wallerman, J., Egberth, M., Larsson, S., Nilsson, L., Eriksson, J., Olsson, H., 2017. A nationwide forest attribute map of Sweden predicted using airborne laser scanning data and field data from the National Forest Inventory. Remote Sens. Environ. 194, 447–454. https://doi.org/10.1016/j.rse.2016.10.022.
Nord-Larsen, T., Schumacher, J., 2012. Estimation of forest resources from a country wide laser scanning survey and national forest inventory data. Remote Sens. Environ. 119, 148–157. https://doi.org/10.1016/j.rse.2011.12.022.
Panagos, P., 2006. The European soil database. GEO: connexion 5, 32–33.
Pecchi, M., Marchi, M., Giannetti, F., Bernetti, I., Binidi, M., Moriondo, M., Maelli, F., Fibbi, L., Corona, P., Travaglini, D., Chirici, G., 2019. Reviewing climatic traits for the main forest tree species in Italy Matteo. iForest Biogeosci. For. 12, 173–180. https://doi.org/10.3832/ifor2835-012.
Persson, H.J., Olsson, H., Soja, M.J., Ulander, L.M.H., Fransson, J.E.S., 2017. Experiences from large-scale forest mapping of Sweden using TanDEM-X data. Remote Sens. 9. https://doi.org/10.3390/rs9121253.
Puletti, N., Floris, A., Scrinzi, G., Chianucci, F., Colle, G., Michelini, T., Pedot, N., Penasa, A., Scalercio, S., Corona, P., 2017. CFOR: a spatial decision support system dedicated to forest management in Calabria. For. - Riv. Di Selvic. Ed Ecol. For. 14, 135–140. https://doi.org/10.3832/efor2363-014.
Rahlf, J., Breidenbach, J., Solberg, S., Næsset, E., Astrup, R., 2014. Comparison of four types of 3D data for timber volume estimation. Remote Sens. Environ. 155, 325–333. https://doi.org/10.1016/j.rse.2014.08.036.
Reese, H., Nilsson, M., Sandström, P., Olsson, H., 2002. Applications using estimates of forest parameters derived from satellite and forest inventory data. Comput. Electron. Agric. 37, 37–55. https://doi.org/10.1016/S0168-1699(02)00118-7.
Särndal, C.-E., Swensson, B., Wretman, J., 2003. Model Assisted Survey Sampling. Springer. ed., Berlin.
Scarascia-Mugnozza, G., Oswald, H., Piussi, P., Radoglou, K., 2000. Forests of the Mediterranean region: gaps in knowledge and research needs. For. Ecol. Manage. 132 (1), 97–109. https://doi.org/10.1016/S0378-1127(00)00381-9.
Smith, P., Bustamente, H., Ahammad, H., Clark, H., Dong, E.A., Elsiddig, H., Haberl, R., Harper, J., House, M., Jafari, O., Masera, C., Mbow, N.H., Racindranath, C.W., Vermeulen, S.J., Campbell, B.M., Ingram, J.S.I., Aide, T.M., Clark, M.L., Grau, H.R., López-Carr, D., Levy, M.A., Redo, D., Bonilla-Moheno, M., Riner, G., Andrade-Núñez, M.J., Muñiz, M., Yale Center for Environmental Law and Policy, FAO, Spracklen, B.D., Kalamandeen, M., Galbraith, D., Gloor, E., Spracklen, D.V., 2016. STATE OF THE WORLD'S FORESTS - agriculture, forestry and other Land use challanges and opportunities, climate change 2014: mitigation of climate change. Contribution of Working Group III to the Fifth Assessment Report of the Intergovernmental Panel on Climate Change. https://doi.org/10.1146/annurev-environ-020411-130608.
Stinson, G., White, J., 2018. What's the Difference Between EFI and NFI? Demystifying current acronyms in forest inventory in Canada.
Stumpf, A., Kerle, N., 2011. Object-oriented mapping of landslides using Random Forests. Remote Sens. Environ. 115, 2564–2577. https://doi.org/10.1016/j.rse.2011.05.013.
Särndal, C.-E., Swensson, B., Wretman, J., 1992. Model Assisted Survey Sampling. Springer, New York 694p.
Tabacchi, G., Di Cosmo, L., Gasparini, P., Morelli, S., 2011. Stima Del Volume E Della Fitomassa Delle Principali Specie Forestali Italiene, Equazioni Di Previsione, Tavole Del Volume E Tavole Della Fitomassa Arborea Epigea.
Tarquini, S., Isola, I., Favalli, M., Mazzarini, F., Bisson, M., Pareschi, M.T., Boschi, E., 2007. TINITALY/01: a new triangular irregular network of Italy. Ann. Geophys. 50, 407–425.
Tarquini, S., Nannipieri, L., 2017. The 10 m-resolution TINITALY DEM as a trans-disciplinary basis for the analysis of the Italian territory: current trends and new perspectives. Geomorphology. https://doi.org/10.1016/j.geomorph.2016.12.022.
Tomppo, E., Olsson, H., Ståhl, G., Nilsson, M., Hagner, O., Katila, M., 2008. Combining national forest inventory field plots and remote sensing data for forest databases. Remote Sens. Environ. 112, 1982–1999. https://doi.org/10.1016/j.rse.2007.03.032.
Waser, L.T., Fischer, C., Wang, Z., Ginzler, C., 2015. Wall-to-wall forest mapping based on digital surface models from image-based point clouds and a NFI forest definition. Forests 6, 4510–4528. https://doi.org/10.3390/f6124386.
Waser, L.T., Ginzler, C., Rehush, N., 2017. Wall-to-Wall tree type mapping from countrywide airborne remote sensing surveys. Remote Sens. 9. https://doi.org/10.3390/rs9080766.
Yu, X., Hyyppä, J., Vastaranta, M., Holopainen, M., Viitala, R., 2011. Predicting individual tree attributes from airborne laser point clouds based on the random forests technique. Isprs J. Photogramm. Remote. Sens. 66, 28–37. https://doi.org/10.1016/j.isprsjprs.2010.08.003.
Zhao, P., Lu, D., Wang, G., Wu, C., Huang, Y., 2016. Examining spectral reflectance saturation in landsat imagery and corresponding solutions to improve forest aboveground biomass estimation. Remote Sens. https://doi.org/10.3390/rs8060469.